Research Article Open Access

Wen-Kai Ge, Gui Lu, Xin Xu, and Xiao-Dong Wang*

Droplet spreading and permeating on the hybrid-wettability porous substrates: a lattice Boltzmann method study

DOI 10.1515/phys-2016-0055 Received Sep 30, 2016; accepted Nov 09, 2016

Abstract: The spreading and permeation of droplets on porous substrates is a fundamental process in a variety of applications, such as coating, dyeing, and printing. The spreading and permeating usually occur synchronously but play different roles in the practical applications. The mechanisms of the competition between spreading and permeation is significant but still unclear. A lattice Boltzmann method is used to study the spreading and permeation of droplets on hybrid-wettability porous substrates, with different wettability on the surface and the inside pores. The competition between the spreading and the permeation processes is studied in this work from the effects of the substrate and the fluid properties, including the substrate wettability, the porous parameters, as well as the fluid surface tension and viscosity. The results show that increasing the surface wettability and the porosity contact angle both inhibit the spreading and the permeation processes. When the inside porosity contact angle is larger than 90° (hydrophobic), the permeation process does not occur. The droplets suspend on substrates with Cassie state. The droplets are more easily to permeate into substrates with a small inside porosity contact angle (hydrophilic), as well as large pore sizes. Otherwise, the droplets are more easily to spread on substrate surfaces with small surface contact angle (hydrophilic) and smaller pore sizes. The competition between droplet spreading and permeation is also related to the fluid properties. The permeation process is enhanced by increasing of surface

tension, leading to a smaller droplet lifetime. The goals of this study are to provide methods to manipulate the spreading and permeation separately, which are of practical interest in many industrial applications.

Keywords: spreading and permeating; lattice Boltzmann method; hybrid wettability; porous substrates

PACS: 68.08.Bc; 68.03.Cd; 47.56.+r.

1 Introduction

The spreading and permeation of droplets on porous substrates is a fundamental process involved in our daily lives and many industrial applications, such as coating [1–4], painting [5, 6], printing [7–10], land pollution control [11, 12], and oil recovery [13]. The spreading and permeation usually occur synchronously but play different roles in the coating or printing applications. Therefore, the spreading and permeation on porous substrates need to be controlled separately. For example, in inkjet printing, the inkjet droplets should permeate as quickly as possible to inhibit the spreading process [7].

The spreading and permeation of droplets on porous substrates has been studied theoretically, experimentally, and numerically. Denesuk et al. [14, 15] studied the spreading and permeation processes on a porous substrate with parallel vertical holes using a simple hydrodynamic model. The process was divided into three stages based on the variety of dominant forces. Davis and Hocking [16, 17] studied the complete and partial wetting of droplets on porous substrates using a modified hydrodynamic model derived from the lubrication approximation. Alleborn and Raszillier [18] investigated the spreading and sorption of a droplet on an anisotropic, layered porous substrate theoretically and numerically. The effects of the porous thickness and the permeability on the sorption process of a sessile droplet were discussed. Espín et al. [19] developed a new lubrication-theory-based model for droplet spreading on permeable substrates that incorporates surface rough-

^{*}Corresponding Author: Xiao-Dong Wang: Research Center of Engineering Thermophysics, North China Electric Power University, Beijing 102206, China; School of Energy Power and Mechanical Engineering, North China Electric Power University, Beijing 102206, China; Email: wangxd99@gmail.com; Tel. and Fax: +86-10-62321277 Wen-Kai Ge, Gui Lu, Xin Xu: Research Center of Engineering Thermophysics, North China Electric Power University, Beijing 102206, China; School of Energy Power and Mechanical Engineering, North China Electric Power University, Beijing 102206, China

ness. Therefore, the model was able to mimic the contactline pinning phenomena observed in experiments. Starov et al. [20] studied the spreading of small liquid drops over thin and thick porous layers in the cases of both complete wetting and partial wetting. The porous substrates in their experiments included nitrocellulose membranes of different porosity and different average pore size, glass, and metal filters. Their study showed that both an effective lubrication and that the liquid exchange between the drop and the porous substrates were equally important. The dynamic contact angle changes rapidly in the initial short stage and then remains at a constant value over the duration of the rest of the spreading process for both the thin and the thick porous substrates. Richard et al. [21] investigated theoretically and experimentally the spreading and penetration of surfactant-laden drops on thin-permeable media with reference to ink-jet printing. They proposed a new model based on energy arguments to describe simultaneous spreading and penetration. They mainly considered the effects of the surfactant concentrations on the spreading and penetration process. Deshpande et al. [22] studied the drop-spreading of silicone oil and polyvinyl alcohol water solution (PVA) droplets on glass and two different kinds of glass fiber mats used in composite processing. Their results show that the volume imbibed into porous media varies linearly with time for polyvinyl alcohol and varies with the square root of time for silicon oil. Different drop sizes were chosen in their experiments to understand the varying effects of driving forces. Among the numerical studies, Neyval et al. [23] use the dimensionless parameter method (wettability, porosity etc.) to study the process of droplets impinging, spreading, and permeating porous substrates. Frank et al. [24, 25] studied the spreading laws of the droplet inertia-controlled stage by changing the wettability and porosity using a lattice Boltzmann method.

Among these studies, most of them [16–19, 22, 23] focused on the permeating process, in which the spreading was neglected. The others [14, 15, 20, 21, 24, 25] studied the spreading and permeating integrally. The separate and competitive mechanisms of the spreading and permeation processes are still unclear, which motivates the present study. In this work, a new method was proposed to tune the spreading-permeation competition of the droplet over the porous substrates. Both the solid and liquid properties are discussed to examine the feasibility of the new method. The goals of this study are to provide methods to manipulate the spreading and permeation separately, which is of practical interest in many industrial applications.

2 Numerical model

The spreading and permeation of droplets on porous substrates is a complex process involving solid-liquid, solid-vapor and liquid-vapor interactions. Therefore, a multiphase lattice Boltzmann method was used to describe the spreading and permeation process, with the capacity of depicting the liquid-vapor replacement process over the substrates, as well as the liquid permeation process into the pores.

2.1 Pseudo-potential LBM model

There are several multiphase lattice Boltzmann models [26–30]. Among these models, the pseudo-potential LBM model [27] proposed by Shan and Chen is a classical approach which is popular in multiphase simulations. In this work, the improved pseudo-potential LBM model [31] is used to model the droplet spreading and permeation processes due to its easy implementation of the fluid-solid interactions. The particle distribution function is based on the Bhatnagar–Gross–Kroot (BGK) approach, which is,

$$f_{\alpha}(\mathbf{x} + \mathbf{e}_{\alpha}\delta t, t + \delta t) = f_{\alpha}(\mathbf{x}, t) - \frac{1}{\tau} \left[f_{\alpha}(\mathbf{x}, t) - f_{\alpha}^{eq}(\mathbf{x}, t) \right]$$
(1)

where $f_{\alpha}(\mathbf{x}, \mathbf{t})$ is the particle distribution function, $\tau = 1$ is the relaxation time and $f_{\alpha}^{\text{eq}}(\mathbf{x}, t)$ is the equilibrium distribution function, which is given by,

$$f_{\alpha}^{\text{eq}}(\mathbf{x}, t) = \rho w_{\alpha} \left[1 + \frac{3}{c^{2}} \mathbf{e}_{\alpha} \cdot \mathbf{u}^{\text{eq}} + \frac{9}{2c^{4}} (\mathbf{e}_{\alpha} \cdot \mathbf{u}^{\text{eq}})^{2} - \frac{3}{2c^{2}} \mathbf{u}^{\text{eq}} \cdot \mathbf{u}^{\text{eq}} \right]$$
(2)

where w_{α} is weighting factor,

$$w_{\alpha} = \begin{cases} 4/9, & \alpha = 0; \\ 1/9, & \alpha = 1, 2, 3, 4; \\ 1/36, & \alpha = 5, 6, 7, 8. \end{cases}$$

In Eqs (1) and (2), e_{α} is the discrete velocity,

$$\mathbf{e}_{\alpha} = \begin{cases} (0,0), & \alpha = 0; \\ (\pm 1,0)c, (0,\pm 1)c, & \alpha = 1,2,3,4; \\ (\pm 1,\pm 1)c, & \alpha = 5,6,7,8; \end{cases}$$

where $c = \delta x/\delta t$ is the lattice velocity, with c = 1. In this paper, the lattice spacing $\delta x = 1$ lu and time step $\delta t = 1$ ts. The macroscopic density is given by

$$\rho = \sum_{\alpha=0}^{8} f_{\alpha}.$$
 (3)

The velocity in equilibrium \mathbf{u}^{eq} is given by

$$\rho \mathbf{u}^{\text{eq}} = \rho \mathbf{u}' + \tau \delta t \mathbf{F}. \tag{4}$$

So the macroscopic fluid velocity **u** can be defined as

$$\rho \mathbf{u} = \rho \mathbf{u}' + \frac{1}{2} \delta t \mathbf{F}, \tag{5}$$

where $\rho \mathbf{u}'$ is given by

$$\rho \mathbf{u}' = \sum_{\alpha=0}^{8} f_{\alpha} \mathbf{e}_{\alpha}. \tag{6}$$

In Eqs (4) and (5), the external force F contains cohesive and adhesive forces, as well as body forces, such as gravity. The cohesive force is calculated by

$$\mathbf{F}_{co}(\mathbf{x}) = -G\psi(\mathbf{x})\sum_{\alpha}w_{\alpha}\psi(\mathbf{x}+\mathbf{e}_{\alpha}\delta t)\mathbf{e}_{\alpha},$$
 (7)

where G is an interaction coefficient, where G < 0 represents attractive force between fluid particles. $\psi(\mathbf{x})$ is equivalent mass. The corresponding equation of state (EOS) for the pseudo-potential model is [31]

$$p = \rho c_s^2 + \frac{1}{2} c_s^2 G \psi^2, \tag{8}$$

where $c_s = 1/\sqrt{3}$ is the lattice sound speed. The equivalent mass can be rearranged with

$$\psi = \sqrt{\frac{2\left(p - \rho c_s^2\right)}{c_s^2 G}}.$$
 (9)

To mimic the high density ratio of the liquid vapor systems, the Redlich-Kwong (R-K) EOS is used to modify the EOS of the pseudo-potential model due to its simplicity [31]. This is given by

$$p = \frac{\rho RT}{1 - b\rho} - \frac{a\rho^2}{\sqrt{T}(1 + b\rho)},\tag{10}$$

where $a = 0.42748R^2T2.5c/p_c$, $b = 0.08664RT_c/p_c$. T_c denotes the critical temperature and p_c is the critical pressure, which can be determined by the given parameters a and b. a, b and T can be tuned to achieve different density ratios.

The adhesive force between the solid and the fluid \mathbf{F}_{ads} can be defined as:

$$\mathbf{F}_{\mathrm{ads}}(\mathbf{x}) = -G\psi(\rho(\mathbf{x})) \sum_{\alpha} w_{\alpha}\psi(\rho_{\mathrm{w}}) s(\mathbf{x} + \mathbf{e}_{\alpha}\delta t) \mathbf{e}_{\alpha}$$
(11)

where *s* is an indicator function that is equal to 1 if the adjacent lattice is solid but 0 for liquid. The fluid viscosity is calculated as $v = 1/3(\tau - 1/2)\delta t$.

2.2 Geometry model

The geometric schematic is shown in Figure 1, which contains 600 × 800 lu². Lattice units are used in the work, in which lu is the lattice unit for length, and ts is the time step for time. The porous substance contains a series of vertical ribs. Only vertical flow occurs when the droplet permeates into the porous substance. All of the ribs have the same height of H=500 lu, an equal width of b', an equal gap of d'. Therefore, the porosity of the substrate is d'/(b'+d'). The droplet is located on the center of the porous substrate (x = 300 lu) with an initial radius of $r_0 = 100 \text{ lu}$.

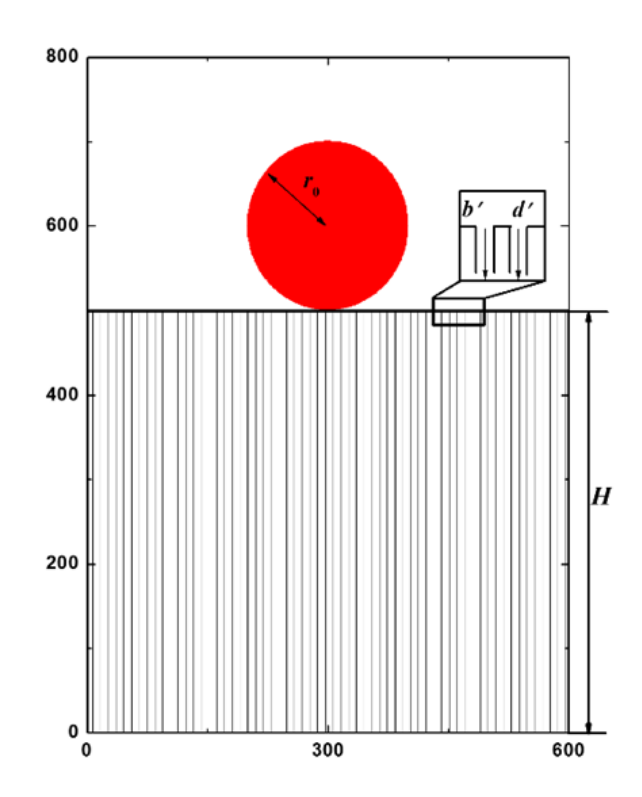


Figure 1: Numerical model schematic.

2.3 Model validation

Figure 2 compares the present LBM simulation with the experimental and the numerical results reported by [22]. In the experiment, the droplet is silicon oil (SO300) with density $\rho = 1040 \text{ kg m}^{-3}$ and surface tension $\sigma = 21 \text{ mN m}^{-1}$. The initial droplet is $r \cdot = 2.61$ mm. The glass fiber porous substrate with unidirectional mat (UDMAT) has a porosity

In the present simulation, a = 2/49, b = 2/21, R = 1, $T/T_c = 0.85$ were chosen for R-K EOS. For the model val486 — W.-K. Ge et al. DE GRUYTER OPEN

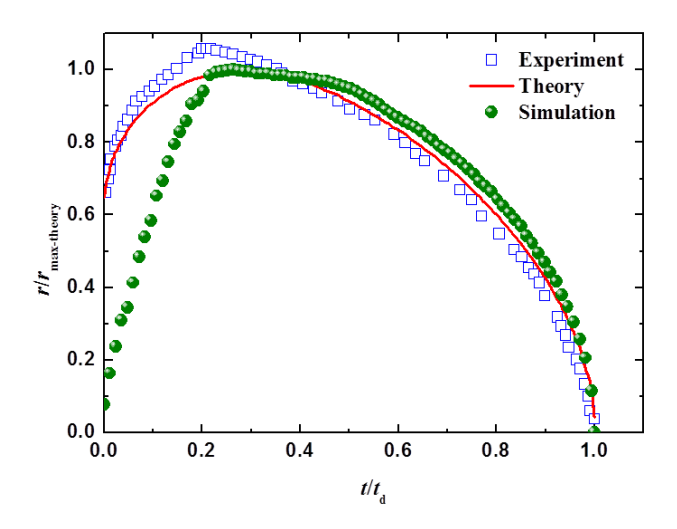


Figure 2: Model validation.

idation calculations, the porous parameters are b'=8 lu for the width and d'=13 lu for the gap, corresponding to a porosity of 0.615. The liquid density is $\rho_l=6.07$ mu lu⁻³, and the vapor density is $\rho_g=0.53$ mu lu⁻³, corresponding to a surface tension of $\sigma=0.16$ mu lu ts⁻². The 'solid density' is $\rho_w=5.124$ mu lu⁻³, corresponding to an equilibrium contact angle of $\theta_{\rm eq}=16.7^{\circ}$. The gravitational acceleration is g=0.0000087 lu ts⁻². Periodic boundary conditions are used in the left and the right sides of the computational region, while bounce-back boundary conditions are adopted on the upper and lower walls.

The LBM results agree well with Kumar's experimental and numerical results when $t/t_d > 0.2$, indicating the capabilities of the pseudo-potential LBM model. It is noted that the simulations diverge with the experimental and numerical results when $t/t_d < 0.2$. The fundamental assumption in the theory plotted in Fig. 2 is the lubrication approximation, which is dealt with a thin liquid film. However, in the present simulation, the initial droplet has perfect roundness with a contact angle of 180° , which is far larger than the small contact angle assumption in the lubrication approximation. In addition, the initial spreading process is controlled by the inertial force, which is also neglected in the theoretical model. As a result, the LBM results deviate from the theoretical prediction and the experimental data when $t/t_d < 0.2$.

3 Results and Discussion

The droplet spreading and permeation processes are driven by the unbalanced Young force (spreading) and the capillary force (permeation). Spreading leads to an in-

crease of the droplet radius while permeation decreases the spreading radius by reducing the droplet volume. Therefore, the spreading law of the droplet on porous substrates is mainly determined by the competition between these two processes. The competition should be controlled by designing appropriate spreading and permeation time scales. In this work, we manipulate the process through both the substrate parameters and the fluid properties.

3.1 Effects of substrate properties

The wettability of porous substrates has been studied in previous works [19, 20, 23–25], however, among which, the substrate surface and the inside pores have unique wettability. To manipulate the spreading and the permeating time scale, we design hybrid wettability characteristics on the substrate surface and the inside pores, for example, hydrophobic surface and hydrophilic inside pores or hydrophilic surface and hydrophilic inside pores. Therefore, the driven forces, both the unbalanced Young force and the capillary force, are different on the substrate surface and the inside pores.

Figure 3 shows snapshots of the droplet spreading and permeating on the porous substrates with equilibrium contact angle of $\theta_{top} = 6^{\circ}$ on the surface and inside pore wettability of (a) $\theta_{inside} = 6^{\circ}$ and (b) $\theta_{inside} = 45^{\circ}$, in which b' = 8 lu and d' = 8 lu. The entire process can be divided into three stages according to the spreading and permeating behaviors. In the first stage, the droplet contacts the porous surface and then spreads to the maximum radius rapidly with little drop permeating into the porous medium. In the second stage, the spreading radius remains constant or slightly decrease since the droplet is pinned at the edge of ribs (column) [32], while the main body of drop permeates into porous medium. In the third stage, the liquid left on the porous surface de-wets and shrinks into the porous medium rapidly, leading to the rapid decrease of the spreading radius.

For the first stage, the inertia and unbalanced Young force dominate the droplet spreading initially, and then the vertical capillary force becomes involved. The vertical capillary force dominates the second stage since the droplet has stopped spreading at this stage. In the last stage, the remaining liquid on the substrate de-wets and shrinks into the porous medium by the capillary force. The de-wetting process occurs at this stage.

Figure 4 shows the variation of droplet radii with time for various substrates with the same surface wettability $(\theta_{top} = 6^{\circ})$ but different wettability of the inside pores. The equilibrium contact angles inside the porous substrate,

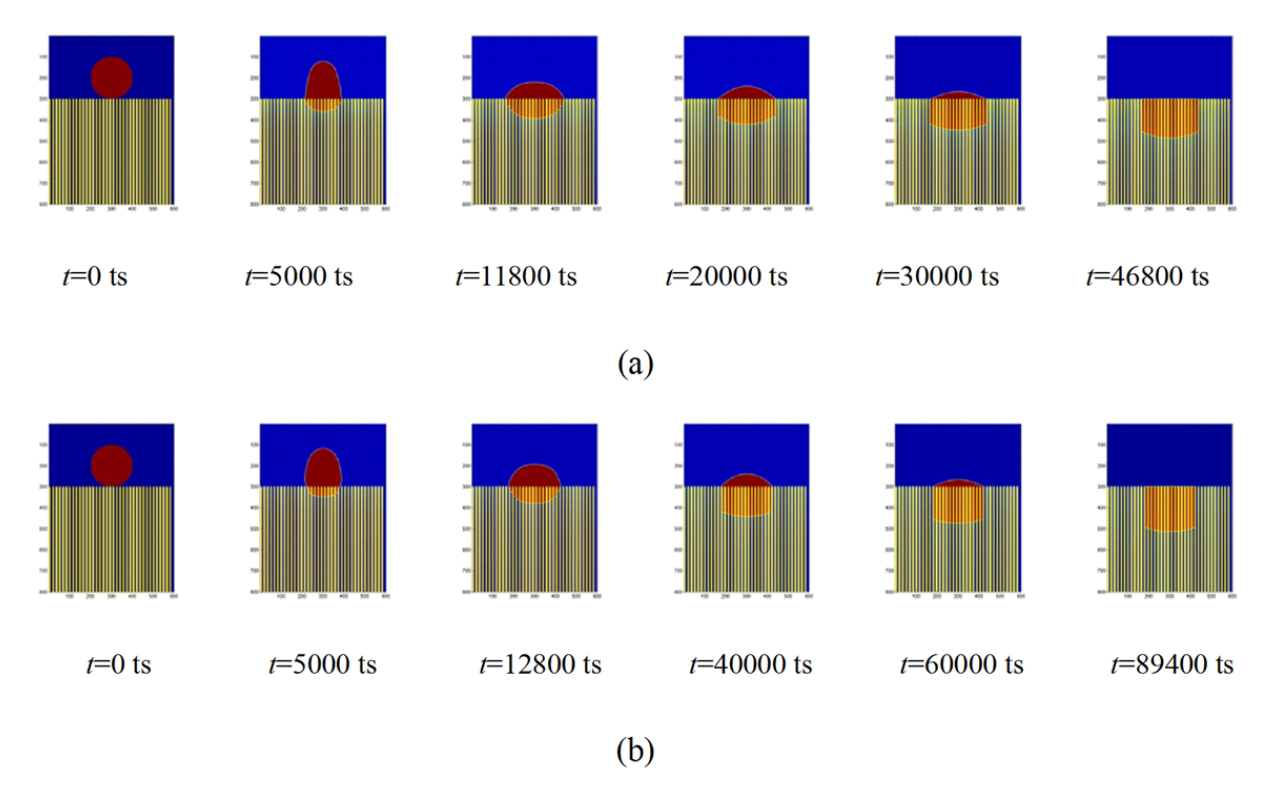


Figure 3: Time evolution of the shape of droplets: (a) $\theta_{inside} = 6'$ and (b) $\theta_{inside} = 45^{\circ}$.

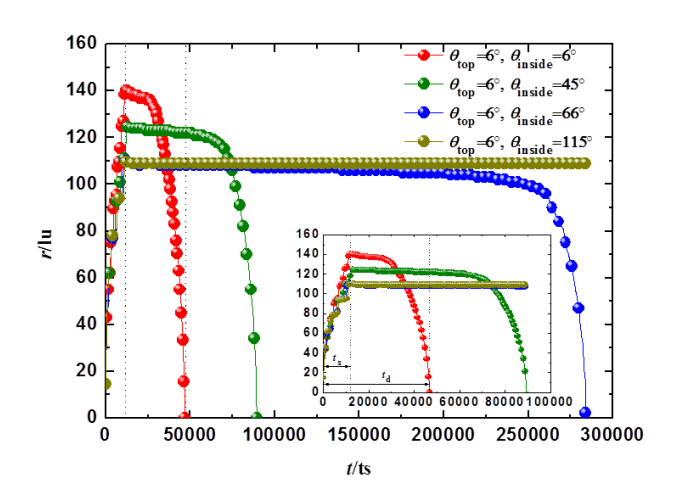


Figure 4: Effects of inside pore wettability on droplet spreading-permeation process ($\theta_{top} = 6^{\circ}$).

 θ_{inside} , range from 6° to 115°. The radius-time curves overlap as a master curve during the fast initial spreading stage since the permeation process does not occur. Increasing the inside pore wettability enhances the permeation of the droplet, leading to a shorter droplet lifetime above the substrates, for example, t=284200 ts for $\theta_{inside}=66^{\circ}$, but t=46800 ts for $\theta_{inside}=6^{\circ}$. It should be noted that permeation is prevented for hydrophobic inside pores with $\theta_{inside}=115^{\circ}$. The spreading droplet suspends on the rib

Table 1: Effects of internal wettability on droplet spreading and permeation.

θ_{top}	θ_{inside}	t_s	t_d	$\lambda = t_s / t_d$	r _{max}
6°	6°	11800	46800	0.252	140
6°	45°	12800	89400	0.143	124.5
6°	66°	11400	284200	0.04	110
6°	115°	12200	∞	0	110

top as in the Cassie stage. As shown in Table 1, the inside pore wettability has little effect on the spreading time scale but greatly affects the permeation time scale. Therefore, the timescale ratio between spreading and permeation decreases with increasing inside pore equilibrium contact angle. The results indicate the feasibility of an approach which tunes the spreading-permeation competition using hybrid-wettability porous substrates.

To further examine the feasibility of the approach, the inside pore wettability is fixed to θ_{inside} = 6° (hydrophilic) while the surface equilibrium contact angles vary from θ_{top} = 6° to θ_{top} = 115° , as shown in Fig. 5 and Table 2. Unlike the cases in Fig. 4, the permeating process occurs in the initial stage due to the small contact angle inside the substrates. Both the spreading rate and maximum spreading radius increase with increasing surface wetta-

488 — W.-K. Ge et al. DE GRUYTER OPEN

Table 2: Effects of surface wettability (θ_{top}) on droplet spreading and permeation.

θ_{top}	θ_{inside}	$t_{\rm s}$	<i>t</i> ,	$\lambda = t_s / t_d$	
	Vinside	LS	t _d	$n - \iota_{s} / \iota_{d}$	r _{max}
6°	6°	11800	46800	0.252	140
45°	6°	11400	54600	0.209	124.5
66°	6°	11400	63200	0.18	108.5
115°	6°	13400	71600	0.187	90

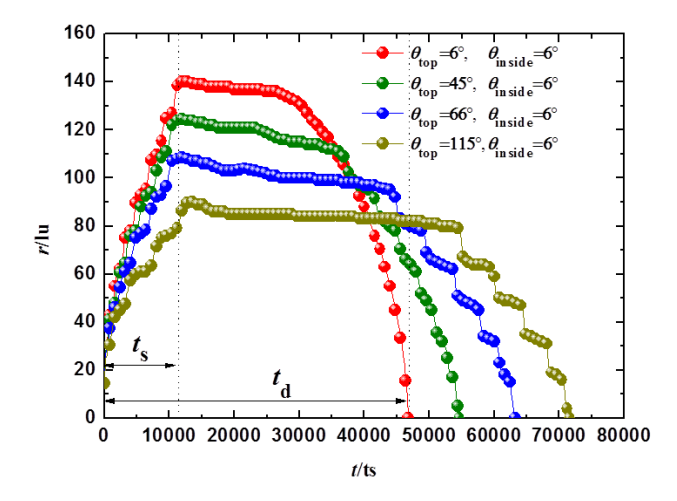


Figure 5: Effects of surface wettability on droplet spreading-permeation process ($\theta_{inside} = 6^{\circ}$).

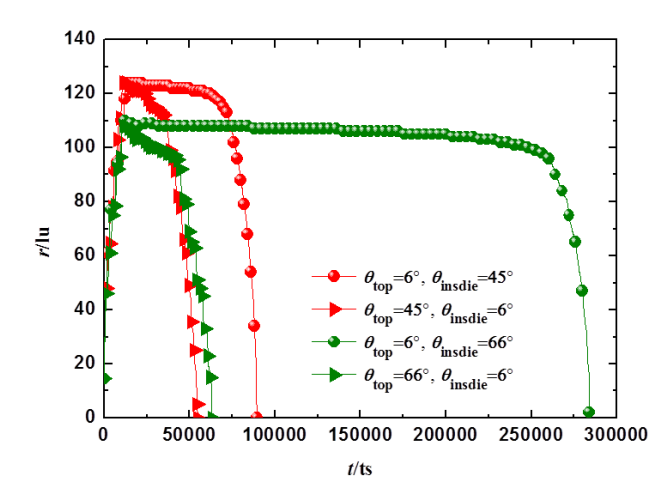


Figure 6: Sensitivity of surface and inside pore wettability on the spreading-permeation process.

bility (from $\theta_{top} = 115^{\circ}$ to $\theta_{top} = 6^{\circ}$). The surface wettability also greatly affects the last de-wetting stage. The remained droplet shrinks more easily on the hydrophilic surfaces with smaller equilibrium contact angle, leading to a faster last stage. In addition, the surface wettability also affects the total droplet lifetime, t_d . With fixed inside pore wettability, the droplet lifetime decreases with increasing sur-

Table 3: Effects of pore sizes on droplet spreading and permeation.

ď	t_s	t_d	$\lambda = t_s / t_d$	r_{max}
8	11600	110200	0.105	109
10	11200	117000	0.096	97
12	11600	117600	0.099	93
14	15600	111600	0.140	92

face wettability. For example, the droplet lifetime is 46800 ts for $\theta_{top} = 6^{\circ}$ but 71600 ts for $\theta_{top} = 115^{\circ}$. For hydrophilic inside pores, permeation affects the spreading of the initial stage, while spreading affects the permeation of the last stage. Both spreading and permeation occur and are coupled. Therefore, the initial spreading can be suppressed by enhancing the wettability of inside pores. The last permeating stage can also be tuned by changing the de-wetting behavior with surface wettability.

Four spreading-permeation scenarios were designed to examine the sensitivity of the surface and inside pore wettability, as shown in Fig. 6. When the inside pore wettability is fixed ($\theta_{inside} = 6^{\circ}$), the variation of surface wettability ($\theta_{top} = 45^{\circ}$ and $\theta_{top} = 66^{\circ}$) has few effects on the spreading-permeation process. The two cases have the same initial spreading rates at the initial stage and the same total droplet lifetime. However, when the surface wettability is fixed as $\theta_{top} = 6^{\circ}$ and the inside pore wettability changes from $\theta_{inside} = 45^{\circ}$ to $\theta_{inside} = 66^{\circ}$, the droplet lifetime increases about three times, from 89400 ts to 284200 ts. The results indicate that the spreading-permeation process is very sensitive to the inside pore wettability.

The pore diameter and the porosity also affect the spreading-permeation process, which is mainly considered by previous studies. The spreading-permeation competition can be also tuned by changing the pore diameter and the porosity, as shown in Table 3, and Figs. 7 and 8, in which the surface and the inside pore have the same equilibrium contact angle. Unlike the hybrid-wettability method shown in Fig. 4, the variation of pore sizes has few effects on spreading-permeation process, which further indicating the feasibility of the method we proposed.

3.2 Effects of fluid properties

The spreading-permeation competition is also affected by fluid properties, as shown in Table 4 and Fig. 9, in which $\theta_{top} = \theta_{inside} = 66^{\circ}$. Both the fluid kinetic viscosity and the surface tension are considered by changing the liquid-vapor density ratio M. The liquid-vapor kinetic viscosity ra-

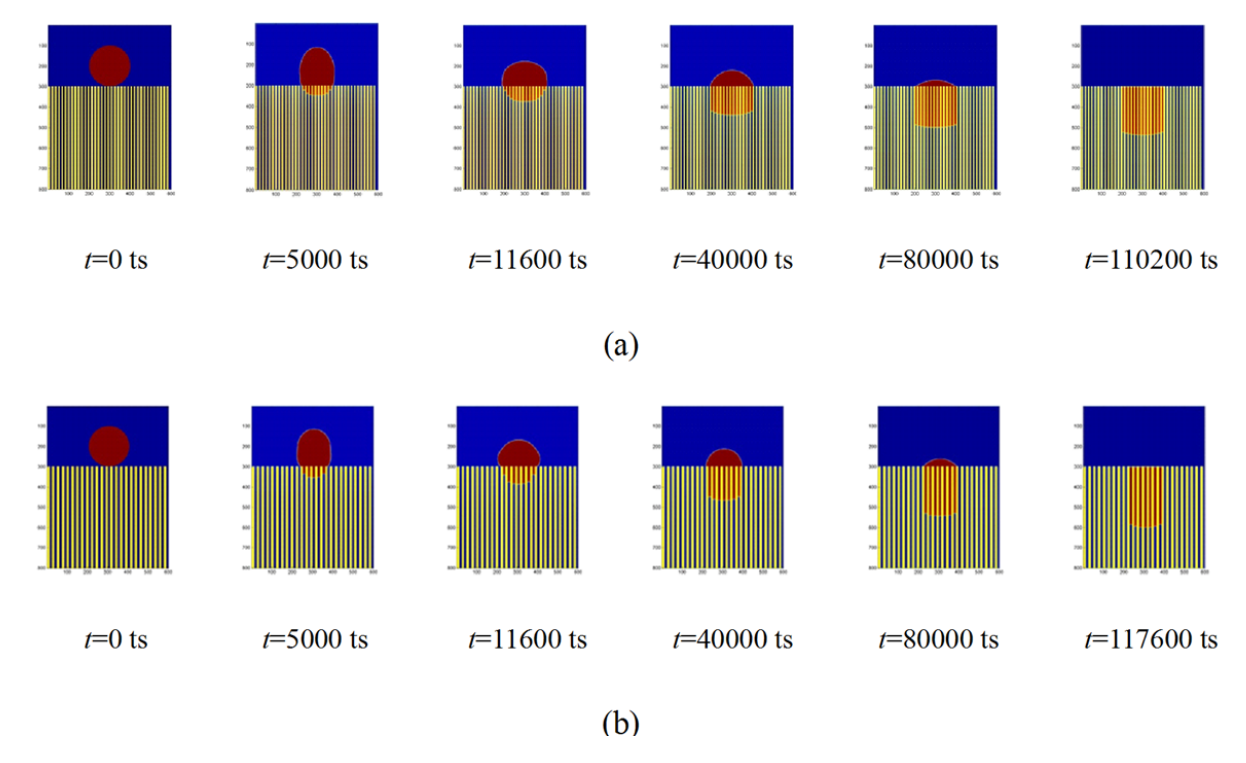


Figure 7: Snapshots of droplet spreading and permeation on porous substrates with different pore sizes: (a) d' = 8 lu and (b) d' = 12 lu.

Table 4: Effects of liquid/vapor density ratio on droplet spreading and permeation.

М	t_s	t_d	$\lambda = t_s / t_d$	r _{max}
5.86	12600	462400	0.027	78
11.45	13600	417600	0.033	92.5
17.56	12000	374000	0.032	94
20.91	11200	323600	0.035	94

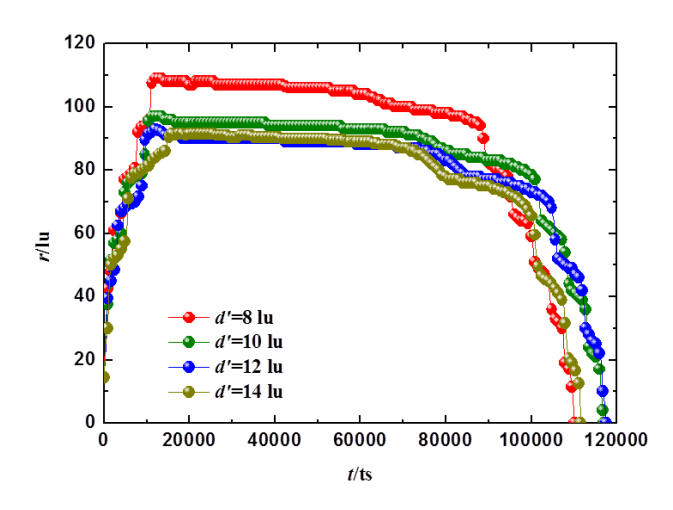


Figure 8: Effects of pore diameters on droplet spreading and permeation on porous substrates.

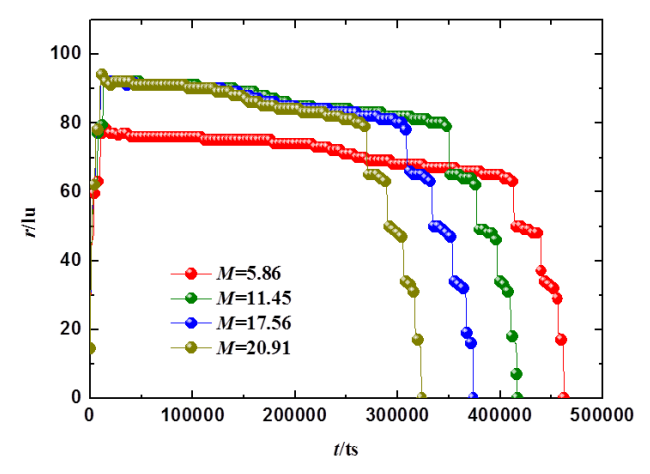


Figure 9: Effects of fluid properties on droplet spreading and permeation on porous substrates.

tio and the surface tension increase with increasing M [33]. The permeating process are enhanced by the increasing of the surface tension, leading to the smaller droplet lifetime [34]. In addition, the variation of fluid properties has fewer effects on the spreading-permeation process than that of solid properties.

4 Conclusions

A new method was proposed to tune the spreadingpermeation competition of a droplet over porous substrates. Both the solid and liquid properties have been discussed to examine the feasibility of the new method. The main conclusions are listed as follows.

- Three stages are observed for the spreadingpermeating process, the initial spreading stage, the permeation dominated stage, and the de-wetting stage. The unbalanced Young force dominates the initial stage and the last de-wetting stage, while the vertical capillary pumping force dominates the middle permeating stage.
- 2. The substrate properties greatly affect the spreading-permeating process. Increasing the surface wettability enhances the spreading rates of the initial stage and the last de-wetting stage, while increasing the inside pore wettability facilitates the permeation process and reduces the droplet lifetime. The spreading-permeation process is more sensitive for the variation of inside pore wettability. The surface and the pore wettability affect the competition greater than the pore size parameters.
- 3. The permeation process is enhanced by increasing of the surface tension, leading to a smaller droplet lifetime. The variation of fluid properties has fewer effects on the spreading-permeation process than that of solid properties.

Acknowledgement: The authors acknowledge financial support from the National Science Fund for Distinguished Young Scholars of China (No. 51525602), the National Science Fund of China (No. 51606064), the Postdoctoral Science Foundation of China (Nos. 2016T90071 and 2015M581046) and the Fundamental Research Funds for the Central Universities (No. 2016MS21).

References

- [1] Bollström R., Määttänen A., Tobjörk D., Ihalainen P., Kaihovirta N., Österbacka R., Peltonen J., Toivakka M., A multilayer coated fiber-based substrate suitable for printed functionality, Org. Electron., 2009, 10, 1020-1023.
- [2] Kim Y. H., Moon D. G., Han J. I., Organic TFT array on a paper substrate, leee. Electr. Device. L., 2004, 25, 702-704.
- [3] P Colombo., Mera G., Riedel R., SorarùG. D., Polymer-derived ceramics: 40 years of research and innovation in advanced ceramics, J. Am. Ceram., Soc., 2010, 93, 1805-1837.

- [4] Blake T. D., Clarke A., Ruschak K. J., Hydrodynamic assist of dynamic wetting, Aiche. J., 1994, 40, 229-242.
- [5] Clarke A., Blake T. D., Carruthers K., A. Woodward, Spreading and imbibition of liquid droplets on porous surfaces, Langmuir., 2002, 18, 2980-2984.
- [6] Holman R. K., Cima M. J., Uhland S. A., Sachs E., Spreading and Infiltration of Inkjet-Printed Polymer Solution Droplets on a Porous Substrate, J. Colloid. Interf. Sci., 2002, 249, 432-440.
- [7] Määttänen, Ihalainen P., Bollström R., Toivakka M., Peltonen J., Wetting and print quality study of an inkjet-printed poly (3hexylthiophene) on pigment coated papers, Colloid. Surface. A., 2010, 367, 76-84.
- [8] Hyväluoma J., Raiskinmäki P., Jäsberg A., Koponen A., Kataja M., Simulation of liquid penetration in paper, J. Timonen, Phys. Rev. E., 2006, 73, 036705
- [9] Oliver J. F., Initial stages of ink jet drop impaction, spreading and wetting on paper, Tappi. J., 1984, 67, 90-94.
- [10] Karnik A.R., Spreading Characteristics of liquids, J. Photogr. Sci., 1977, 25, 197-201.
- [11] Roberts D., Griffiths R. F., A model for the evaporation of droplets from sand, Atmos. Environ., 1995, 29, 1307-1317.
- [12] Griffiths R. F., Roberts I. D., Droplet evaporation from porous surfaces; model validation from field and wind tunnel experiments for sand and concrete, Atmos. Environ., 1999, 33, 3531-3549.
- [13] Mohammed M., Babadagli T., Wettability alteration: A comprehensive review of materials/methods and testing the selected ones on heavy-oil containing oil-wet systems, Adv. Colloid. Interfac., 2015, 220, 54-57.
- [14] Denesuk M., Smith G.L., Zelinski B.J.J., Kreidl N.J., Uhlmann D.R., Capillary penetration of liquid droplets into porous materials, J. Colloid. Interf. Sci., 1993, 158, 114-120.
- [15] Denesuk M., Zelinski B.J.J., Kreidl N.J., Uhlmann D.R., Dynamics of incomplete wetting on porous materials, J. Colloid. Interf. Sci., 1994, 168, 142-151.
- [16] Davis S. H., Hocking L. M., Spreading and imbibition of viscous liquid on a porous base, Phys. Fluids., 1999, 11, 48-57.
- [17] Davis S. H., Hocking L. M., Spreading and imbibition of viscous liquid on a porous base. II, Phys. Fluids., 2000, 12, 1646-1655.
- [18] Alleborn N., Raszillier H., Spreading and sorption of a droplet on a porous substrate, Chem. Eng. Sci., 2004, 59, 2071-2088.
- [19] Espin L., Kumar S., Droplet spreading and absorption on rough, permeable substrates, J. Fluid. Mech., 2015, 784, 465-486.
- [20] Starov V. M., Zhdanov S. A., Kosvintsev S. R., Sobolev V. D., Velarde M. G., Spreading of liquid drops over porous substrates, Adv. Colloid. Interfac., 2003, 104, 123-158.
- [21] Daniel R. C., Berg J. C., Spreading on and penetration into thin, permeable print media: Application to ink-jet printing, Adv. Colloid. Interfac., 2006, 123, 439-469.
- [22] Kumar S. M., Deshpande A. P., Dynamics of drop spreading on fibrous porous media, Colloid. Surface. A., 2006, 277, 157-163.
- [23] Reis N. C., Griffiths R. F., Santos J. M., Parametric study of liquid droplets impinging on porous surfaces, Appl. Math. Model., 2008, 32, 341-361.
- [24] Frank X., Perré P., Droplet spreading on a porous surface: A lattice Boltzmann study, Phys. Fluids., 2012, 24, 042101.
- [25] Frank X., Perré P., Li H. Z., Lattice Boltzmann investigation of droplet inertial spreading on various porous surfaces, Phys. Rev. E., 2015, 91, 052405.
- [26] Gunstensen K., Rothman D. H., Zaleski S., Zanetti G., Lattice Boltzmann model of immiscible fluids, Phys. Rev. A., 1991, 43,

- 4320-4317.
- [27] Shan X.W., Chen H. D., Lattice Boltzmann model for simulating flows with multiple phases and components, Phys. Rev. E., 1993, 47, 1815-1820.
- [28] Swift M. R., Orlandini E., Osborn W. R., Yeomans J. M., Lattice Boltzmann simulations of liquid-gas and binary fluid systems, Phys. Rev. E., 1996, 54, 5041-5052.
- [29] He X. Y., Chen S. Y., Zhang R. Y., A Lattice Boltzmann Scheme for Incompressible Multiphase Flow and Its Application in Simulation of Rayleigh-Taylor Instability, J. Comput. Phys., 1999, 152, 642-663.
- [30] Zu Y. Q., He S., Phase-field-based lattice Boltzmann model for incompressible binary fluid systems with density and viscosity contrasts, Phys. Rev. E., 2013, 87, 043301-043301.

- [31] Yuan P., Schaefer L., Schaefer. Equations of state in a lattice Boltzmann model, Phys. Fluids., 2006, 18, 042101.
- [32] Alava M. J., Dubé M., Droplet spreading and pinning on heterogeneous substrates, Phys. Rev. E., 2012, 86, 3461-3463.
- [33] Huang H., Li Z., Liu S., Lu X., Shan-and-Chen-type multiphase lattice Boltzmann study of viscous coupling effects for twophase flow in porous media, Int. J. Numer. Meth. Fl., 2009, 61, 341-354.
- [34] Taghilou M., Rahimian M. H., Investigation of two-phase flow in porous media using lattice Boltzmann method, M. Comput. Math. Appl., 2014, 67, 424-436.